PAPER Special Section on Heterostructure Microelectronics with TWHM 2009

Analysis of Passivation-Film-Induced Stress Effects on Electrical Properties in AlGaN/GaN HEMTs

Naoteru SHIGEKAWA[†a)] *and* Suehiro SUGITANI[†], *Members*

SUMMARY Effects of stress in passivation films on the electrical properties of (0001) AlGaN/GaN HEMTs are numerically analysed in the framework of the edge force model with anisotropical characteristics in elastic properties of group-III nitrides explicitly considered. Practical compressive stresses in passivation films induce negative piezoelectric charges below the gates and bring forth a-few-volt shallower threshold voltages. In addition, the shift in the threshold voltage due to the compressive stress is proportional to $L_G{}^{-1.1\sim-1.5}$ with gate length L_G, which is comparable to the expectation based on the charge balance scheme. These result suggest that passivation films with designed stress might play a crucial role in realising AlGaN/GaN HEMTs with shallow or positive threshold voltages.

key words: *GaN, HEMT, threshold voltage, piezoelectric effects, film stress*

1. Introduction

Due to their high breakdown voltage and excellent transport properties, AlGaN/GaN HEMTs are promising devices for high-frequency and high-power applications. HEMTs with shallower or positive threshold voltages V_{th}'s have been eagerly sought so as to fully exploit their potential. A variety of structures for realising such HEMTs, such as *p*-type doped gates [1], MIS-like heterostructures [2], InGaN-cap layers [3], and stressed InAlN barriers [4], have been explored.

It was shown that V_{th} in GaAs MESFETs largely changed when the mechanical stress of their passivation films was varied. The change in the threshold voltage ΔV_{th} was explained by a scheme in which the difference in stresses between gates and the neighbouring passivation films (i) caused the concentration of mechanical forces at the edges of gates on semiconductor surfaces (edge force), (ii) induced the non-uniform stress and hence piezoelectric charges in the MESFET channels, and (iii) shifted the V_{th} [5], [6]. It was suggested that V_{th} in AlGaN/GaN HEMTs was shifted by means of a similar mechanism [3], [7], [8].

In recent "More Moore, More Than Moore" era, the non-uniform stress has been positively exploited in the cutting-edge Si VLSI technologies so as to enhance the transport properties of carriers. Processes for controlling stresses in passivation films in the 45-nm CMOS platform were separately optimised for *n*- and *p*-MOSFETs so that the on-current-to-off-current ratios of both devices were simultaneously improved [9].

Manuscript received November 20, 2009.
Manuscript revised February 18, 2010.
[†]The authors are with NTT Photonics Laboratories, NTT Corporation, Atsugi-shi, 243-0198 Japan.
a) E-mail: shige@aecl.ntt.co.jp
DOI: 10.1587/transele.E93.C.1212

We previously analysed the impact of the stress in passivation films on V_{th} of HEMTs formed on (0001) AlGaN/GaN heterostructures by using the edge force model [10]. Given that the piezoelectric effects vanish in elastically-isotropic materials [11], we explicitly considered the anisotropic characteristics of the elastic properties [12], [13] of group-III nitrides in order to retain the consistency in the analysis. We found that V_{th} of AlGaN/GaN HEMTs was sensitive to the stress in the passivation films and thick passivation films with compressive stress might be useful for realising HEMTs with shallower or positive V_{th}'s.

In this paper, we first give a full description of methods that we previously employed. Next we investigate the impact of the edge forces on the distribution of piezoelectric charges, the potential profile, and ΔV_{th}, with emphasis on their dependencies on the gate length. Then we discuss the possibility of scaling of these piezoelectric-effect-based phonomena in case that the passivation films are compressively-stressed.

2. Method

We consider AlGaN/GaN Schottky diodes with Schottky contacts (gates) sandwiched by passivation films with mechanical stress. The length of parts covered by the passivation films is 1.0 μm. The thickness d_{AlGaN} and Al content of AlGaN barrier are 20 nm and 0.25, respectively. The concentration of residual donors in the GaN channel and the concentration of two-dimensional electron gas (2DEG) in the unbiased heterostructure are assumed to be $1\times10^{15}\,\mathrm{cm}^{-3}$ and $1\times10^{13}\,\mathrm{cm}^{-2}$, respectively. We place acceptor-like surface states on the surface of the AlGaN barriers. Their density is preset to be $1\times10^{13}\,\mathrm{cm}^{-2}\,\mathrm{eV}^{-1}$ [14]. Values of parameters characterizing the elastic, electric, and piezoelectric properties of heterostructures are taken from a literature [15].

We assume that

i. the passivation films are elastically uniform, i.e., the stress in passivation films $\sigma_{f,0}$ is independent of position,
ii. the stress of gates is negligibly small in comparison with that of passivation films,
iii. the piezoelectric constants and elastic compliances of AlGaN are the same as those of GaN,
iv. the electric field in heterostructures does not cause the stress, i.e., the reverse piezoelectric effects are negligi-

bly small, and

v. the quantum-mechanical characteristics of carriers are ignorable.

On these assumptions, the stress in media covering heterostructures (passivation films and gates) $\sigma_f(x_1)$is approximately expressed as

$$\sigma_f(x_1) = \begin{cases} \sigma_{f,0} & (|x_1| > L_G/2) \\ 0. & \text{(others)} \end{cases} \tag{1}$$

Here x_1 denotes the coordinate along the gate-to-ohmic direction, and $x_1 = \pm L_G/2$ indicates the locations of the edges. The gate length of diodes is given by L_G. The centre of gates is placed at $x_1 = 0$. The coordinates along the gate-width direction and along the vertical direction are denoted as x_2 and x_3, respectively.

The x_1-derivative of σ_f gives a force loaded on the heterostructure surface p, which is given by

$$p = \sigma_{f,0} d_f \{\delta(x_1 - L_G/2) - \delta(x_1 + L_G/2)\}, \tag{2}$$

where d_f is the thickness of passivation films. Note that p is concentrated at the edges between gates and passivation films on the heterostructure surfaces (the edge force) since σ_f is a step function of x_1. It is noteworthy that $\sigma_{f,0}$ is negative (positive) when the stress in the passivation films is compressive (tensile). The structure investigated in this work is schematically shown in Fig. 1 for the case of compressive passivation films.

The edge force induces stress inside of the heterostructures, which is denoted by a second-rank tensor σ. The stress tensor is related to the strain γ (second-rank tensor), the electric field E (vector), the electric displacement D (vector), and spontaneous polarization P_{sp} (vector) through the following constitutive equations:

$$\sigma = C\gamma - eE \cong C\gamma, \tag{3}$$

$$D = e\gamma + \epsilon E + P_{sp} \cong eC^{-1}\sigma + \epsilon E + P_{sp}. \tag{4}$$

Here C, e, and ϵ are the elastic stiffness (fourth-rank tensor), piezoelectric constant (third-rank tensor), and dielectric constant (second-rank tensor), respectively. The rightmost expressions in the above equations are due to the assumption that the reverse piezoelectric effects are negligible.

The concentration of piezoelectric charges due to the stress, minus the divergence of the polarization P induced by σ, is given by

$$-\mathrm{div}P = -\mathrm{div}[eC^{-1}\sigma]. \tag{5}$$

We estimate the distribution of the edge-force-based σ and the resultant piezoelectric charges by using the method summarized in the Appendix. Next, we numerically solve the Poisson equation of the heterostructure with these piezoelectric charges considered and obtain the band structure and the distribution of 2DEG for a given bias voltage V_b. We define V_{th} by extrapolating the relationship between the concentration of 2DEG at the centre of gates n_s and V_b to the limit of $n_s = 0\,\mathrm{cm}^{-2}$ [5].

3. Results

3.1 Piezoelectric Charges and Potential Profiles

The distribution of piezoelectric charges in half of diodes with (L_G, $\sigma_{f,0}d_f$) = (0.5 μm, −0.5 GPa·μm) is shown in

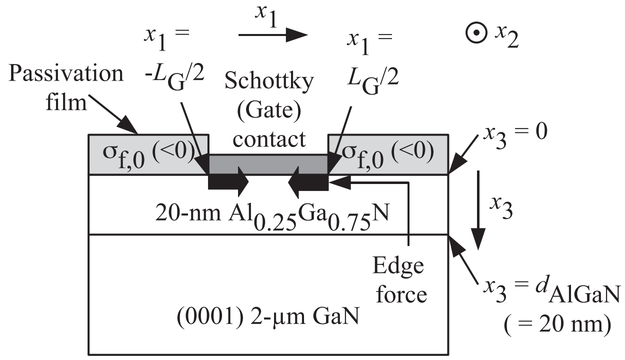

Fig. 1 Schottky diodes composed of stress-free gates sandwiched by passivation films with mechanical stress. The direction of the edge force, which is loaded at the edges $x_1 = \pm L_G/2$, is shown for the compressively-stressed passivation films.

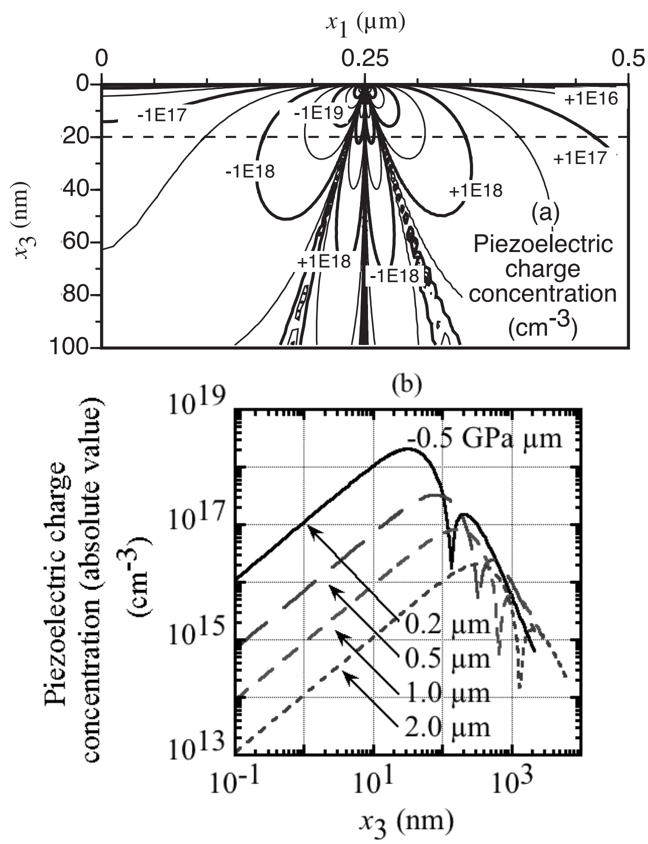

Fig. 2 (a): The concentration of piezoelectric charges induced in a 0.5-μm diode for $\sigma_{f,0}d_f = -0.5\,\mathrm{GPa}\cdot\mu\mathrm{m}$. The dashed lines at $x_3 = 20\,\mathrm{nm}$ shows the AlGaN/GaN heterointerface. (b): The concentration of piezoelectric charges at the centre of gates in 0.2, 0.5, 1.0, and 2.0-μm diodes for $\sigma_{f,0}d_f = -0.5\,\mathrm{GPa}\cdot\mu\mathrm{m}$.

Fig. 2(a). The interface between the AlGaN barriers and GaN channels is shown by a dashed line. Note that $\sigma_{f,0}d_f$ of $-0.5\,\text{GPa}\cdot\mu\text{m}$ corresponds to 1-μm thick passivation films with a compressive stress of 0.5 GPa ($5\times10^9\,\text{dyn/cm}^2$), which is practically achievable [16]. It is found that negative charges with a concentration of $\sim 10^{16-18}\,\text{cm}^{-3}$ emerge around the centre of gates ($x_1 = 0\,\mu\text{m}$). Positive charges with a similar concentration appear in a region below the passivation films. In addition, the concentration of the piezoelectric charges diverges to $\pm\infty$ in the vicinities of the edges ($x_1 = 0.25\,\mu\text{m}$). Note that the sign of charges at the respective positions is inverted when the stress in the passivation films is tensile.

Figure 2(b) compares distribution of piezoelectric charges along the x_3 direction at the centre of gates for L_G = 0.2, 0.5, 1.0, and 2.0 μm with $\sigma_{f,0}d_f$ of $-0.5\,\text{GPa}\cdot\mu\text{m}$. The peak closer to (farther from) the surface in each distribution profile is due to negative (positive) charges. We find that the piezoelectric charges are distributed more deeply for longer gate lengths.

The contours of the conduction-band minimum E_C in unbiased diodes with (L_G, $\sigma_{f,0}d_f$) = (0.2 μm, $-0.5\,\text{GPa}\cdot\mu\text{m}$), (0.5 μm, $-0.5\,\text{GPa}\cdot\mu\text{m}$), and (1.0 μm, $-0.5\,\text{GPa}\cdot\mu\text{m}$) are shown in Figs. 3(a), 3(b), and 3(c), respectively. Bold lines in the respective figures are for $E_C = 0\,\text{eV}$, which corresponds to the Fermi energy. Figure 4 compares profiles of E_C at the centre of unbiased gates and n_s for (L_G, $\sigma_{f,0}d_f$) = (0.5 μm, 0 GPa$\cdot\mu$m) and (0.5 μm, $-0.5\,\text{GPa}\cdot\mu\text{m}$). This figure shows that E_C in the GaN channels is raised and n_s changes from 10.03×10^{12} to $6.67\times10^{12}\,\text{cm}^{-2}$ when the compressive edge force of is loaded. In addition, as is seen from Figs. 3(a), 3(b), and 3(c), E_C at the AlGaN/GaN interface in the vicinities of edges is $> 0\,\text{eV}$ and there appears regions with $E_C < 0\,\text{eV}$ in AlGaN barriers. Such changes in E_C are more marked in diodes with shorter gates.

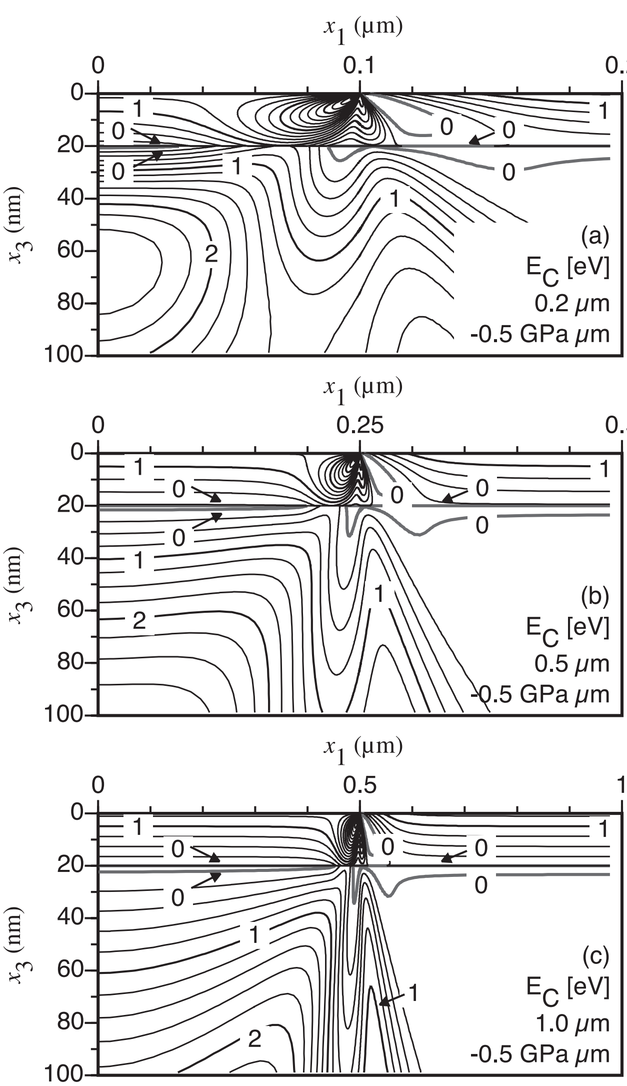

Fig. 3 The contours of the conduction-band minimum of unbiased diodes with (L_G, $\sigma_{f,0}d_f$) = (a) (0.2 μm, $-0.5\,\text{GPa}\cdot\mu\text{m}$), (b) (0.5 μm, $-0.5\,\text{GPa}\cdot\mu\text{m}$), and (c) (1.0 μm, $-0.5\,\text{GPa}\cdot\mu\text{m}$).

3.2 Shift in Threshold Voltages

Figure 5(a) shows the relationship between n_s and the bias voltage V_b for the 0.5-μm diode with different values of $\sigma_{f,0}d_f$ between 0.5 and $-0.5\,\text{GPa}\cdot\mu\text{m}$. We find that n_s changes almost linearly with V_b for each $\sigma_{f,0}d_f$ so that V_{th} is extracted with accuracy by extrapolating the n_s-V_b relation. Then we define the shift in the threshold voltage due to the edge force ΔV_{th}, which is hereafter referred to as $\Delta V_{th,\text{no 2DEG limit}}$.

Figure 5(b) shows $\Delta V_{th,\text{no 2DEG limit}}$ for the 0.5-μm diode. In this diode V_{th} increases (gets shallower) by $\approx$ 1.2 V when $\sigma_{f,0}d_f$ changes from 0 to $-0.5\,\text{GPa}\cdot\mu\text{m}$. It decreases (gets deeper) by $\approx$ 1.8 V when $\sigma_{f,0}d_f$ changes from 0 to $0.5\,\text{GPa}\cdot\mu\text{m}$.

Figures 6(a) and 6(b) show the relationships between $\Delta V_{th,\text{no 2DEG limit}}$ and L_G for $\sigma_{f,0}d_f$ of $-0.1\,\text{GPa}\cdot\mu\text{m}$ and $-0.5\,\text{GPa}\cdot\mu\text{m}$, respectively. We find by means of least-square fitting that $\Delta V_{th,\text{no 2DEG limit}}$ is approximately proportional to $L_G^{-1.5}$ and $L_G^{-1.1}$ for $\sigma_{f,0}d_f$ of $-0.1\,\text{GPa}\cdot\mu\text{m}$ and

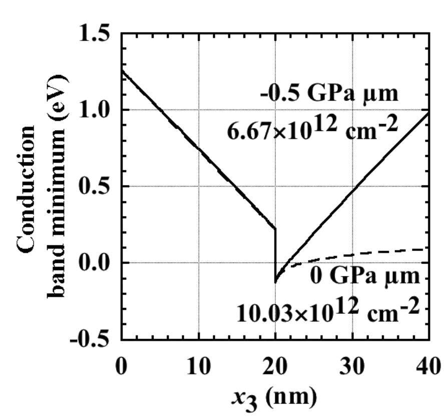

Fig. 4 The profiles of the conduction-band minimum at the centre of unbiased diodes with (L_G, $\sigma_{f,0}d_f$) = (0.5 μm, 0 GPa$\cdot\mu$m) and (0.5 μm, $-0.5\,\text{GPa}\cdot\mu\text{m}$). The concentration of 2DEG for each band profile is also shown.

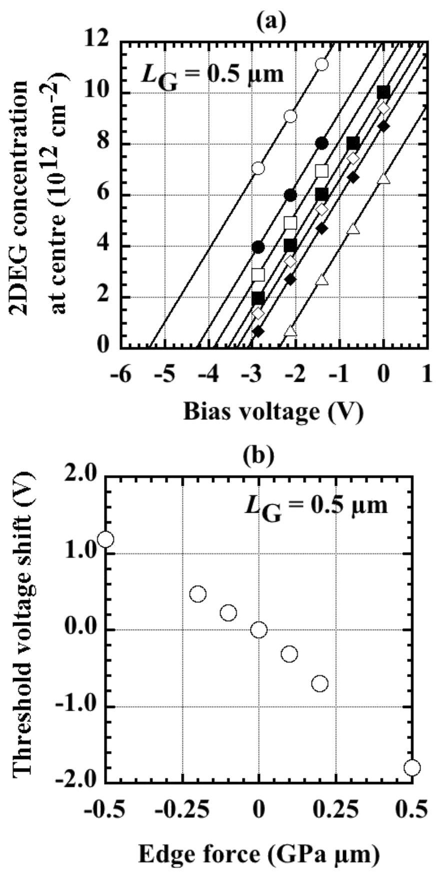

Fig. 5 (a) Relationships between the 2DEG concentration at the centre of gate in a 0.5-μm diode and bias voltage for $\sigma_{f,0}d_f$ of 0.5, 0.2, 0.1, 0, −0.1, −0.2, and −0.5 GPa · μm (from top to bottom). (b) The shift in V_{th} due to the edge force in a 0.5-μm diode.

−0.5 GPa·μm, respectively. These results qualitatively agree with the report that the shift in V_{th} due to the tensile stress in passivation films was larger in shorter-gate devices [7].

4. Discussion

4.1 Threshold Voltage Shift in Charge Balance Scheme

By using the scheme that the balance of charges determines the concentration of 2DEG in AlGaN/GaN heterostructures [17], the shift in the threshold voltage, denoted as $\Delta V_{th,\text{ charge balance}}$, is expressed as

$$\Delta V_{th,\text{ charge balance}} = -Q_{\text{piezo}}/(\epsilon_{33}/d_{\text{AlGaN}}), \tag{6}$$

where Q_{piezo} and ϵ_{33} are the sheet concentration of piezoelectric charges in the GaN channels at the centre of gates and the dielectric constants along the x_3 axis, respectively.

We obtain at the centre of gates

$$\int_{d_{\text{AlGaN}}}^{\infty} \partial_1\sigma_{13}dx_3 \sim \frac{\sigma_{f,0}d_f d_{\text{AlGaN}}^2}{{L_G}^3},$$
$$\int_{d_{\text{AlGaN}}}^{\infty} \partial_3\sigma_{11}dx_3 = \sigma_{11}|_{d_{\text{AlGaN}}}^{\infty} \sim \frac{\sigma_{f,0}d_f}{L_G}, \text{ and} \tag{7}$$

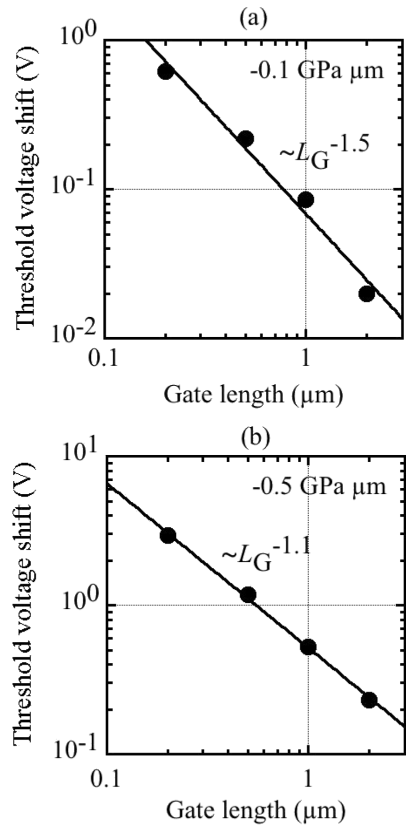

Fig. 6 Relationships between the shift in threshold voltage and gate lengths (a) for $\sigma_{f,0}d_f$ =-0.1 GPa · μm, and (b) for $\sigma_{f,0}d_f$ =-0.5 GPa · μm.

$$\int_{d_{\text{AlGaN}}}^{\infty} \partial_3\sigma_{33}dx_3 = \sigma_{33}|_{d_{\text{AlGaN}}}^{\infty} \sim \frac{\sigma_{f,0}d_f d_{\text{AlGaN}}^2}{{L_G}^3},$$

by using Eq. (A· 3). Hence, by using Eq. (A· 4), Q_{piezo} is scaled as

$$|Q_{\text{piezo}}| = \left|\int_{d_{\text{AlGaN}}}^{\infty}(-\text{div}P)dx_3\right| \sim \frac{|\sigma_{f,0}|d_f}{L_G}\left(1 + O\left(\frac{d_{\text{AlGaN}}}{L_G}\right)^2\right). \tag{8}$$

Here $O((\frac{d_{\text{AlGaN}}}{L_G})^2)$ indicates that a higher-order term is in the order of $(d_{\text{AlGaN}}/L_G)^2$ and negligibly small. Equation (8) suggests that in the charge balance framework both Q_{piezo} and $\Delta V_{th,\text{ charge balance}}$ are likely to be proportional to $\sigma_{f,0}d_f/L_G$.

The charge balance scheme is likely to be justifiably applied for estimating ΔV_{th} when (i) the piezoelectric charges are localized in the vicinities of the AlGaN/GaN interfaces, and (ii) the variation of the potential profile at the centre of gates along the normal direction is much more marked than its variation along the in-plane direction, i.e., the long-channel approximation is valid. We confirmed by analysing data shown in Figs. 3(a), 3(b), and 3(c) that magnitude of the second derivative of E_C with respect to x_3 $|\partial_{33}E_C|$ is $\gg |\partial_{11}E_C|$ at the centre of gates in the GaN channels (not depicted), which suggests that the second requirement should be fulfilled. However, the piezoelectric charges are distributed inside of GaN channels, and their distribution is deeper for longer gate lengths, as is shown in Fig. 2(b), which is likely to qualitatively explain why $\Delta V_{th,\text{ no 2DEG limit}}$ more rapidly decreases than $\Delta V_{th,\text{ charge balance}}$ when the gate length increases.

Anyhow the result that the dependence of $\Delta V_{th,\text{ no 2DEG limit}}$ on the gate length is expressed as $\Delta V_{th,\text{ no 2DEG limit}} \sim L_G{}^m$ with the exponent m of $-1.1{\sim}-1.5$, indicating that the threshold voltages in HEMTs with shorter gates are more sensitive to the edge forces, is consistent with more marked change in E_C in the GaN channels for shorter gate lengths. In addition, it is noteworthy that the value of exponent m is close to that expected by means of the charge balance framework ($m = -1$), which suggests that the threshold voltage of HEMTs with stressed passivation films might be controllable by more precisely modelling the relationships among stresses, potential profiles, and threshold voltages.

4.2 Singularities Due to the Edge Force Model

Given that regions with $E_C > 0$ eV appear at the AlGaN/GaN interface in the vicinities of edges with compressively-stressed passivation films [Figs. 3(a), 3(b), and 3(c)], the 2DEG is assumed to be depleted there. This means that the 2DEG should be confined at the AlGaN/GaN interface between the two edges. Hence the heterostructures with strained passivation films might provide platforms for realising nanodevices such as nanowires and single electron transistors. It is also found that there appears parts with $E_C < 0$ eV in the AlGaN barriers in the vicinity of the edges. Such parts might cause gate leakage.

The spatial variation in E_C in the vicinities of edges is likely to be enhanced by the anomaly in the concentration of the piezoelectric charges [Fig. 2(a)], which is due to the singularity of the stress there [Eq. (A· 3)]. It is noteworthy that the singularity of the stress inevitably occurs in the framework of the edge force model in which the passivation films are assumed to be infinitely rigid.

However, actual the passivation films are equipped with the finite rigidity and their mechanical stress is likely to be smoothly varied around the edges [18]. Hence the singularity in the stress and the anomaly in the piezoelectric charges should vanish. Possible changes in the spatial variation of E_C and in the concentration of the piezoelectric charges due to the finite rigidity in the passivation films should be investigated for quantitatively discussing possibilities of the 2DEG confinement and the gate leakage. Measurements of channel potentials in AlGaN/GaN interfaces around the edges as well as those of elastic properties of passivation films may provide useful informations for examining these issues.

5. Conclusion

We numerically analysed the impact of the non-uniform stress in Schottky diodes on (0001) AlGaN/GaN heterostructures on their electrical properties by using the edge force model. The edge force was assumed to be due to the passivation films with mechnical stress and stress-free Schottky (gate) contacts. The anisotropic characteristics in elastic properties of group-III nitrides were explicitly considered. We found that due to practical compressive stresses in passivation films, negative piezoelectric charges with a concentration of $\sim 10^{16\sim18}\,\text{cm}^{-3}$ emerged and the conduction-band minimum was raised in GaN channels below the gates, so that the threshold voltage increased (got shallowed) by a few volts. We also found that the shift in the threshold voltage was approximately proportional to $L_G{}^{-1.1\sim-1.5}$, which was close to expectation from the charge balance scheme ($\Delta V_{th}{\sim}L_G{}^{-1}$). These results suggest that passivation films with designed compressive stresses might be applicable for controlling the characteristics of AlGaN/GaN HEMTs and realising shallow or positive threshold voltages.

Acknowledgments

The authors are grateful to Dr. Takatomo Enoki for his fruitful discussions and encouragements.

References

[1] Y. Uemoto, M. Hikita, H. Ueno, H. Matsuo, H. Ishida, M. Yanagihara, T. Ueda, T. Tanaka, and D. Ueda, "Gate injection transistor (GIT) — A normally-Off AlGaN/GaN power transistor using conductivity modulation," IEEE Trans. Electron Devices, vol.54, no.12, pp.3393–3399, 2007.

[2] T. Oka and T. Nozawa, "AlGaN/GaN recessed MIS-Gate HFET with high-threshold-voltage normally-off operation for power electronics applications," IEEE Electron Device Lett., vol.29, no.7, pp.668–670, 2008.

[3] T. Mizutani, M. Ito, S. Kishimoto, and F. Nakamura, "AlGaN/GaN HEMTs with thin InGaN cap layer for normally off operation," IEEE Electron Device Lett., vol.28, no.7, pp.549–551, 2007.

[4] M. Hiroki, N. Maeda, and T. Kobayashi, "Electrical properties and device characteristics of InAlN/AlGaN/AlN/GaN heterostructure field effect transistors," Physica Status Solidi (c), DOI: 10.1002/pssc.200880970, 2009.

[5] P.M. Asbeck, C.-P. Lee, and M.-C.F. Chang, "Piezoelectric effects in GaAs FET's and their role in orientation-dependent device characteristics," IEEE Trans. Electron Devices, vol.ED-31, no.10, pp.1377–1380, 1984.

[6] T. Onodera and H. Nishi, "Theoretical study of the piezoelectric effect on GaAs MESFET's on (100), (011), and ($\bar{1}\bar{1}\bar{1}$)Ga, and (111)As substrates," IEEE Trans. Electron Devices, vol.36, no.9, pp.1580–1585, 1989.

[7] R.A. Davies, D.Z. Bazley, S.K. Jones, H.A. Lovekin, W.A. Phillips, R.H. Wallis, J.C. Birbeck, T. Martin, and M.J. Uren, "The gate-length dependent performance of AlGaN/GaN HFETs with silicon nitride passivation," Proc. 2000 8th IEEE International Symposium on High Performance Electron Devices for Microwave and Optoelectronic Applications, pp.76–81, Glaskow, UK, 2000.

[8] H. Ishida, T. Murata, M. Ishii, Y. Hirose, Y. Uemoto, T. Tanaka, and D. Ueda, "Experimental and theoretical examination of orientation effect on piezoelectric charge at gate periphery in AlGaN/GaN HFETs," IEEE Trans. Electron Devices, vol.53, no.7, pp.1524–1529, 2006.

[9] T. Miyashita, et al., "High-performance and low-power bulk logic

platform utilizilng FET specilfic multilple-stressors wilth highly enhanced strailn and full-porous low-k interconnects for 45-nm CMOS technology," Tech. Digest IEEE International Electron Device Meeting 2007, pp.251–254, Washington DC, 2007.

[10] N. Shigekawa and S. Sugitani, "Numerical analysis of impact of stress in passivation films on electrical properties in AlGaN/GaN heterostructures," IEICE Electronics Express, vol.6, no.14, pp.1045–1050, 2009.

[11] J.F. Nye, Physical Properties of Crystals, Clarendon Press, Oxford, 1957.

[12] S.G. Lekhnitskii, Anisotropic Plates, translated from the second Russian edition by S.W. Tsai and T. Cheron, Gordon and Breach Science Publishers, New York-London-Paris, 1968.

[13] C.E. Murray, "Mechanics of edge effects in anisotropic thin film/substrate systems," J. Appl. Phys., vol.100, no.10, 103532, 2006.

[14] S. Barbet, R. Aubry, M.-A. di Forte-Poisson, J.-C. Jacquet, D. Deresmes, T. Mélin, and D. Théron, "Surface potential of n- and p-type GaN measured by Kelvin force microscopy," Appl. Phys. Lett., vol.93, no.21, 212107, 2008.

[15] O. Ambacher, J. Smart, J.R. Shealy, N.G. Weimann, K. Chu, M. Murphy, W.J. Schaff, L.F. Eastman, R. Dimitrov, L. Wittmer, M. Stutzmann, W. Rieger, and J. Hilsenbeck, "Two-dimensional electron gases induced by spontaneous and piezoelectric polarization charges in N- and Ga-face AlGaN/GaN heterostructures," J. Appl. Phys., vol.85, no.6, pp.3222–3233, 1999.

[16] E.Y. Chang, G.T. Cibuzar, and K.P. Pande, "Passivation of GaAs FET's with PECVD silicon nitride films of different stress states," IEEE Trans. Electron Devices, vol.35, no.9, pp.1412–1418, 1988.

[17] J.P. Ibbetson, P.T. Fini, K.D. Ness, S.P. DenBaars, J.S. Speck, and U.K. Mishra, "Polarization effects, surface states, and the source of electrons in AlGaN/GaN heterostructure field effect transistors," Appl. Phys. Lett., vol.77, no.2, pp.250–252, 2000.

[18] A. Fischer, H. Kühne, B. Roos, and H. Richter, "Elastic strain relaxation in patterned heteroepitaxial structures," Semicond. Sci. Technol., vol.9, no.12, pp.2195–2198, 1994.

Appendix: Edge-Force Based Piezoelectric Charges in Elastically Anisotropic Channels

The anisotropic characteristics in elastic properties of (0001) GaN channels are analysed by solving the following equation:

$$\beta_{11}\mu^4 + (2\beta_{13} + \beta_{55})\mu^2 + \beta_{33} = 0, \qquad \text{(A·1)}$$

where in GaN channels with $6mm$ symmetry $\beta_{11} = S_{11} - (S_{12})^2/S_{11}, \beta_{13} = S_{13} - S_{12}S_{13}/S_{11}, \beta_{33} = S_{33} - (S_{13})^2/S_{11}$, and $\beta_{55} = S_{44}$, respectively, by using the elastic compliance in matrix notation S_{ij}, the inverse of C. Values of β_{ij} for GaN are shown in Table A·1. Equation (A·1) gives four pure imaginary solutions $\mu = \pm ic$ and $\pm id$ $(c, d > 0)$. In the present case, we obtain $c = 1.695$ and $d = 0.575$. Note that in the isotropic materials $\beta_{13} = S_{12} - S_{12}^2/S_{11}$, $\beta_{33} = S_{11} - (S_{12})^2/S_{11}$, and $\beta_{55} = 2(S_{11} - S_{12})$ so that $c = d = 1$.

The stress in channels due to the edge force $\sigma_{f,0}d_f\delta(x_1 - L_G/2)$ is given by the following equations:

Table A·1 The coefficients β_{ij} for (0001) GaN channels.

(i,j)	(1,1)	(1,3)	(3,3)	(5,5)
β_{ij} [10^{-3} GPa^{-1}]	2.950	−0.8321	2.799	11.11

$$\begin{aligned}
\sigma_{11} &= -\frac{\sigma_{f,0}d_f(c+d)x_{1'}^3}{\pi[x_{1'}^2 + c^2x_3^2][x_{1'}^2 + d^2x_3^2]},\\
\sigma_{13} &= -\frac{\sigma_{f,0}d_f(c+d)x_{1'}^2x_3}{\pi[x_{1'}^2 + c^2x_3^2][x_{1'}^2 + d^2x_3^2]}, \quad \text{and} \qquad \text{(A·2)}\\
\sigma_{33} &= -\frac{\sigma_{f,0}d_f(c+d)x_{1'}x_3^2}{\pi[x_{1'}^2 + c^2x_3^2][x_{1'}^2 + d^2x_3^2]},
\end{aligned}$$

where $x_{1'} \equiv x_1 - L_G/2$. Furthermore we obtain σ_{22} by using the constraint that the channel is not strained along the x_2 direction:

$$\sigma_{22} = -\frac{S_{12}\sigma_{11} + S_{13}\sigma_{33}}{S_{11}}. \qquad \text{(A·3)}$$

By citing non-zero elements of the elastic compliance tensor C and the piezoelectric tensor e in GaN and using Eq. (5), $-\text{div}P$ is written as

$$\begin{aligned}
-\text{div}P = \frac{e_{15}}{C_{44}}\partial_1\sigma_{13} - \frac{-e_{31}C_{33} + e_{33}C_{13}}{C_{11}C_{33} - C_{13}^2}\partial_3\sigma_{11}\\
-\frac{e_{31}C_{13} - e_{33}C_{11}}{C_{11}C_{33} - C_{13}^2}\partial_3\sigma_{33}, \qquad \text{(A·4)}
\end{aligned}$$

where $\partial_k\sigma_{ij}$ is the x_k-derivative of σ_{ij}. We add the contribution of the force loaded at the other edge $(x_1 = -L_G/2)$ to $-\text{div}P$ and estimate the concentration of the piezoelectric charges in Schottky diodes.

Naoteru Shigekawa received the B.S., M.S., and Ph.D. degrees in physics from the University of Tokyo, Japan, in 1984, 1986, and 1993, respectively. He joined Atsugi Electrical Communications Laboratories, Nippon Telegraph and Telephone Corporation (NTT), Kanagawa, Japan, in 1986, and was engaged in research of hot carrier transport in III-V compound-semiconductor heterostructures. From 1993 to 1994, he was a Visiting Scientist at the Department of Physics, University of Nottingham, U.K., where he worked on resonant-tunnelling heterojunction bipolar transistors. Currently, he is with NTT Photonics Laboratories, Kanagawa. His current research interests are transport properties in compound semiconductor heterostructures and electron devices. Dr. Shigekawa is a member of the Physical Society of Japan, the Japan Society of Applied Physics, the American Physical Society, the Institute of Physics, and IEEE.

Suehiro Sugitani received the B.E. and M.E. degrees in electronics engineering from Kyushu University, Fukuoka, Japan, in 1983 and 1985, respectively. He joined the NTT Atsugi Electrical communication Laboratory, Kanagawa, Japan, in 1985. Since then, he has been engaged in research and development on fabrication technology for high-speed GaAs MESFET's and IC's, and three-dimensional interconnect technology for GaAs MMIC's. Since 2000, he has studied and developed fabrication technology for ultra-high-speed InP-based IC's. He is currently a Senior Research Engineer at the NTT Photonics Laboratories. Mr. Sugitani is a member of the Japan Society of Applied Physics.